

How to Cite:

Vajravelu, A., Tamilselvan, K. S., Mahadi, M., Zaki, W. S. B. W., Suresh, K. S., & Iyer, G. G. (2022). Development of 3-stage hybrid computer aided design (3-HCAD) system for multi-modal medical images to identify brain tumor. *International Journal of Health Sciences*, 6(S6), 7576–7590. <https://doi.org/10.53730/ijhs.v6nS6.11392>

Development of 3-stage hybrid computer aided design (3-HCAD) system for multi-modal medical images to identify brain tumor

Ashok Vajravelu

Faculty of Electrical and Electronic Engineering, Universiti Tun Hussein Onn Malaysia, Malaysia

K. S. Tamilselvan

Department of ECE, KPR Institute of Engineering and Technology, Anna University, Coimbatore, India

*Corresponding author email: kstamilselvan@gmail.com

Orchid id: 0000-0001-8364-0596

Dr. Muhammad Mahadi

Faculty of Electrical and Electronic Engineering, Universiti Tun Hussein Onn Malaysia, Malaysia

Dr. Wan Suhaimizan Bin Wan Zaki

Faculty of Electrical and Electronic Engineering, Universiti Tun Hussein Onn Malaysia, Malaysia

K. S. Suresh

Head (Technology Extension Division), Centre for Development of Imaging Technology (C-DIT), Thiruvananthapuram, India

Gowtham G. Iyer

PhD Scholar (GE210002), Faculty of Electrical and Electronic Engineering, Universiti Tun Hussein Onn Malaysia, Malaysia

Abstract---The latest developments in medical imaging and computer-aided solutions for image processing problems attract attention of various researchers to impart their research in the medical imaging field. Designing and developing efficient algorithms to present the medical information effectively have become critical areas of research in this field. A 3-Stage Hybrid Computer Aided Design system is introduced to identify Brain tumor in earlier stages by extracting meaningful information from multimodal medical images. The preferred multi-modality images is Magnetic Resonance Imaging (MRI) and Computed Tomography (CT). The CAD system proposed in this

paper can eliminate the dependency on human operators as it is an efficient software-based system. The first stage in this model consists of image pre-processing with Wavelet and Curvelet transforms. The second stage of the CAD system is an image segmentation process, which involves a combination of Wavelet Transform and Watershed Technique. The third stage involves image fusion, where the individually segmented CT and MRI images are fused together to obtain an integrated complementary information from two different images. This is followed by decomposing CT and MRI images using the Dual Tree Complex Wavelet Transform (DTCWT) and Nonsubsampled Contourlet Transform (NSCT). Simulation results indicate that this proposed 3-HCAD system using multi-modal medical images performs better than existing hybrid systems. A clinical study with 30 patients has been executed with the proposed algorithm and the sorting results are used to compare efficiency with previous findings. It is shown that the proposed 3-HCAD system results in increased accuracy and sensitivity.

Keywords--hybrid computer aided design, magnetic resonance imaging, computed tomography, dual tree complex wavelet transform, nonsubsampled contourlet transform.

Introduction

In India, according to estimates published in *American Society of Clinical Oncology* on July 16, 2021, around 13, 92,179 people are diagnosed with cancer every year and 70% of this count result in fatality. This ratio shows that fewer than 30 per cent of Indian patients diagnosed with cancer live five years or longer after the diagnosis (Mathur et al., 2020). As per the American Brain Tumor Association (ABTA), 700,000 people in the US are affected by primary brain tumor. About 120 types of brain tumors have been found around the globe (Arizmendi et al., 2012). In order to reduce the impact of brain tumor, it is essential to diagnose it in its earlier stages and to provide proper treatment (Bauer et al., 2011; Chawla et al., 2009; Ashok & Kumar, 2013). This increases the significance of research in the medical imaging field to design and develop effective systems to address this severe problem. The proposed 3-HCAD system has been applied on real time clinical images from 30 patients. Derived results are compared with results from applying existing algorithms, published in previous years, on the same set of images.

Proposed 3-Stage Hybrid Computer Aided Design (3-HCAD) System

A 3-Stage Hybrid Computer Aided Design (3-HCAD) system that applies on multi-modal medical images to identify brain tumor in earlier stages is illustrated in Figure 1. The first stage of the proposed 3-HCAD system involves image pre-processing, using wavelet transform and curvelet transform. The pre-processing steps fine tune the contrast control level, which in turn provides better enhanced imaging and likewise brings out the significant details present in the original tumor image for more relevant interpretation (Portilla et al., 2003). The denoised

and enhanced clinical CT and MRI images are suitable inputs for the succeeding phase of the CAD system. The next stage of the proposed system is segmentation of the enhanced image for isolating the tumor from its background tissues and bones. In order to accomplish this, a hybrid algorithm using a combination of Wavelet Transform along with Watershed method is used. The third stage of the proposed CAD system is image fusion, which fuses the individually segmented CT and MRI images to obtain integrated complementary information from two different image modalities. The resultant output is more precise, effective and enlightening than the individual CT and MRI images (Mitchell, 2010). This can be achieved by decomposing CT and MRI images using the Dual Tree Complex Wavelet Transform (DTCWT) and Nonsubsampled Contourlet Transform (NSCT) (Yang et al., 2014; Ashok et al., 2010). Fusion process is applied on the decomposed images and they are reconstructed using inverse transform. The new fused image has more information content.

Hybrid Preprocessing Technique

Preprocessing or denoising is a technique which is used to recover the original image U from an observation V , when the original image has been degraded by a noise component N . This can be mathematically expressed as $V=U+N$ (Padma & Sukanesh, 2011).

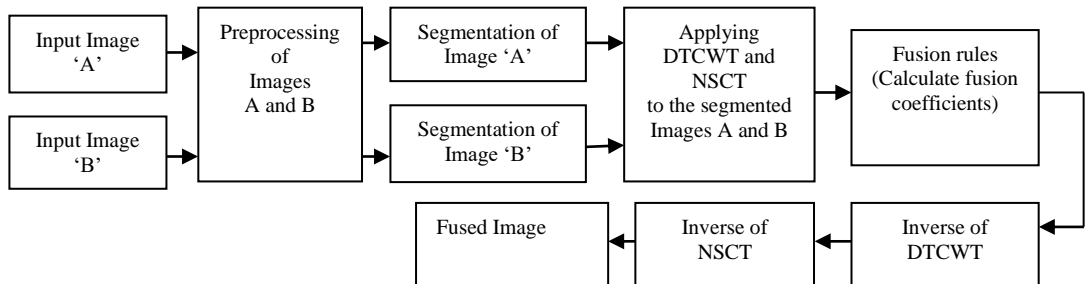


Fig 1. Block diagram of 3-Stage Hybrid Computer Aided Design System

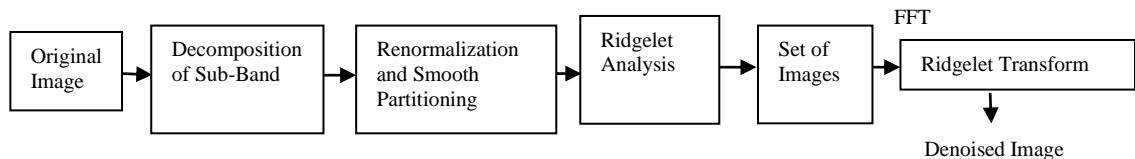


Fig 2. Block diagram of image denoising using Curvelet

A novel method for image denoising is used which involves a combination of two mathematical transforms, Wavelet and Curvelet. For homogeneous areas, wavelet is suitable and for edge detection, curvelet transform will be preferred (Vidyapeetham, 2010). Haar wavelet is used in this application with two level decompositions. The primary step of denoising using wavelet transform is the Thresholding step (Kumar and Verma, 2012).

Noise reduction using Wavelet Transform

Denoising and Compression, which are special features of the Wavelet transform, are preferred techniques used in image processing applications (Chang et al., 2000; Om & Biswas, 2012). Denoising is a process in which a real signal X is recovered from a noisy signal N with an observation Y . Denoising is mathematically represented in equation (2.1).

$$Y = X + N \quad (2.1)$$

The computed value of estimation is illustrated by equation (2.2),

$$B = \{g_m\}, m < N < 0 \text{ as } X = \sum_{m=0}^{N-1} \sigma_m(\langle X, g_m \rangle) g_m \quad (2.2)$$

where, σ_m is the thresholding function which eliminates noise signal in the transform domain while protecting the real signal (Vidyapeetham, 2010). The threshold level parameter T plays an important role (Dhillon et al., 2018). There are several ways to find the value of 'T' including hard, soft, affine, global and level-dependent thresholding methods. Level-Dependent Threshold is adopted in this research.

Denoising using Curvelet Transform

Curvelet transform is suitable for images with curves due to its multi-scale representation (Akbarzadeh et al., 2014; Ashok et al., 2011). Curvelet denoising includes four stages of operations as shown in Figure 2. These four-stages result in high PSNR and low MSE for the images (Starck et al., 2002). The four stages of curvelet based image denoising are explained in detail in the following section.

Sub-band decomposition

$$f \mapsto (P_0 f, \Delta_1 f, \Delta_2 f, \dots) \quad (2.3)$$

As per equation (2.3), if the given image is divided into different layers, then every layer is constituted of different frequencies where:

P_0 indicates low pass filtering and

$\Delta_1, \Delta_2 \dots$ indicate band pass filtering action.

Equation (2.4) illustrates the decomposition of sub bands.

$$P_0 f = \Phi_0 * f \quad \Delta_s f = \Psi_{2s} * f \quad (2.4)$$

Reconstruction of the original image can be expressed as given in equation (2.5).

$$f = P_0(P_0 f) + \sum_s \Delta_s(\Delta_s f) \quad (2.5)$$

Energy preservation

Energy preservation is done as per expression (2.6).

$$\|f\|_2^2 = \|P_0 f\|_2^2 + \sum_s \|\Delta_s f\|_2^2 \quad (2.6)$$

Smooth partitioning

The windowing function w is non-negative and smooth (AlZubi, 2011; Sivaranjani et al., 2019). The energy content of this function can be portioned using the relationships (2.7) and (2.8).

The energy of certain pixel (x, x_2) is divided between all sampling windows of the grid.

$$\sum_{k_1, k_2} w^2(x_1 - k_1, x_2 - k_2) \equiv 1 \quad (2.7)$$

$$\sum_{Q \in Q_s} w_Q^2 \equiv 1 \quad (2.8)$$

Reconstruction

The function can be reconstructed using equation (2.9) as shown below:

$$\sum_{Q \in Q_s} w_Q \cdot h_Q = \sum_{Q \in Q_s} w_Q^2 \cdot h = h \quad (2.9)$$

Ridgelet analysis

Ridgelet is an orthonormal set $\{\rho_n\}$ for $L^2(\mathbb{R}^2)$ developed by Candès & Donoho (1998). In the frequency domain, the ridgelet component can be represented as per the equation (2.10).

$$\hat{\rho}_\lambda(\xi) = \frac{1}{2} |\xi|^{-1} \left(\hat{\psi}_{j,k}(|\xi|) \cdot \omega_{i,l}(\theta) + \hat{\psi}_{j,k}(-|\xi|) \cdot \omega_{i,l}(\theta + \pi) \right) \quad (2.10)$$

Where, ω_i is the repeated wavelets for the range $[-\pi, \pi]$, i and $l \in [0, 2^{i-1}-1]$ are angular scale and angular location respectively, $\psi_{j,k}$ represents the Meyer wavelet and j and k are the ridgelet scale and ridgelet location respectively.

Performance Analysis of Image Preprocessing

The proposed image denoising technique is simulated with a suitable software tool and the simulation results are shared here. These simulation results are further compared with existing filtering techniques, such as wiener filter and median filter and algorithms like non-local image denoising and wavelet based denoising techniques. Table 1 shows the comparison of parameters including SNR, SD and Median for different denoising techniques. The comparison is also

done between filtering and histogram equalization methods for each technique (Abdullah et al., 2007; Jeyashanthi, & Ashok, 2010).

Table 1
Comparison of parameters for various Image Preprocessing Techniques

Technique	Signal to Noise Ratio		Standard Deviation		Median	
	Filtered	Hist. Equalized	Filtered	Hist. Equalized	Filtered	Hist. Equalized
Median Filter	1.843	3.1250	3.5e+002	3.3e+002	26	124
Curvelet Technique	3.1420	3.8612	2.6e+002	2.7e+002	24	123
Wavelet Transform	3.984	4.3514	3e+002	3e+002	22	125
Non-local Algorithm	4.2368	4.9104	2.6e+002	2.5e+002	23	126
Proposed Method	4.517	5.368	2.2e+002	2.2e+002	21	128

Wavelet and Watershed based Segmentation

Image Segmentation is a technique used to isolate the region of interest from the source image for better analysis of the required region.

Proposed Image Segmentation Technique

The various stages of the proposed segmentation method are image pre-processing, image segmentation and extraction of features. In the pre-processing step, image enhancement is done using wavelet technique. Watershed technique is used in the segmentation phase. In the feature extraction stage, the Root Mean Square Error (RMSE), Peak Signal to Noise Ratio (PSNR) and Average Difference (AD) are computed.

Image Segmentation

The watershed transformation method is generally perceived as a more complicated segmentation operation compared to other image segmentation techniques. But it is still used in several applications due its segmentation efficiencies (AlZubi et al., 2011; Ashok et al., 2010). This method is especially useful in the medical field due to its capability to resolve overlapping of the closest gray levels, typical in medical images. In this proposed model, the watershed technique is used for segmenting images. The image is split into different grey level-based areas and the resultant image is converted into a graphical representation (Padma & Sukanesh, 2011; Ashok & Murugesan, 2017).

Feature Extraction and Evaluation of Efficiency

The accuracy as well as the segmentation efficiency of the system is measured with the help of signal to noise ratio, average difference and root mean square error.

Performance Analysis of Segmentation Process

Totally thirty images were selected for analysis. The proposed segmentation technique was examined on MRI and CT brain images collected from Q-Scans in Erode, Tamil Nadu, India. The results tested using MATLAB tool are listed in Figure 3. Sample of normal MR image and image with tumor are shown in Figures 3(a) and 3(b). The contrast is enhanced as in Figure 3(c). Figure 3(d) shows the image with 2-level decomposition. Figures 3(e) indicates the extracted LL section with wavelet transform to separate the tumor from its background. Reconstructed image with extracted boundary is shown in Figure 3(f).



Fig 3. Sample images and results of segmented MRI Image: (a) Sample of normal MR image (b) Sample tumor MR image (c) Image with contrast enhancement (d) Image with 2-level decomposition (e) LL section extracted image with wavelet transform (f) Image reconstructed with watershed algorithm.

For the values obtained from the proposed model, PSNR has maximum value and AD has minimum value.

Novel Combined Approach of Dual Tree Complex Wavelet Transform (DTCWT) and Nonsubsampled Contourlet Transform (NSCT) based Image Fusion

Image fusion is the technique of obtaining the required information from multi modal images, applied majorly in the fields of medical imaging, remote sensing and satellite imaging (Mahidar et al., 2011; Dhavan & Garg, 2014; Sivaranjani et al., 2018). The main objective of image fusion is to separate the information of our interest in an image and to combine similar information to get a more exact and effective representation in a single fused image (Shreyamsha, 2015). In the medical arena, image fusion process provides abundant data to doctors and radiologists to diagnose critical diseases (Bai & Jin, 2015; Ashok et al., 2011). The main focus in this area of research is to continuously improve performance of image fusion techniques that is measured using some indicators such as Root Mean Square Error, Average Difference, Peak Signal To Noise Ration, etc. In order to attempt improvement of these indicators over existing image fusion techniques (pixel based, pyramid based and wavelet based techniques), a new hybrid technique which uses a combination of Dual Tree Complex Wavelet Transform (DTCWT) and non sub sampled Contourlet Transform (NSCT) is proposed. The shift invariance property in DTCWT is achieved in DWT by increasing the sampling rate by two times. This can be achieved in DTCWT by removing the down sampled image after the initial level filtering (Bhonsle & Dewangan, 2012;

Mahidar et al., 2011). The NSCT is a special type of Contourlet Transform that includes a shift invariant technique.

Dual Tree Complex Wavelet Transform (DTCWT)

The Dual Tree Complex Wavelet Transform (DTCWT) is a complex valued extension of the standard wavelet. It uses a special type of filtering technique called as Complex valued filtering which decomposes the given input image into real and imaginary parts. These real and imaginary parts give the magnitude and phase information (Mahidar et al., 2011; Ashok et al., 2018). Then for each pair of sub bands the sum and difference are calculated (Bai & Jin, 2015). Implementation of the complex 2-D dual-tree can be expressed as:

$$(hx+jgx)(hy+jgy) = (hx.hy-gx.gy) + j (hx.gy+gx.hy) \quad (4.1)$$

DTCWT provides better directional selectivity than DWT. With DTCWT selectivity is increased in six directions including $\pm 15^\circ$, $\pm 45^\circ$, $\pm 75^\circ$ while 0° , 45° and 90° are the only sub band directions for DWT as shown in Figure 4.

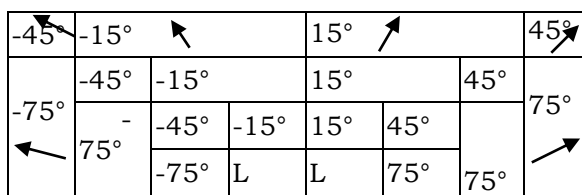


Fig 4. Orientation labeled sub bands of Complex Wavelet Transform

Nonsubsampled Contourlet Transform (NSCT)

NSCT is a combination of Nonsubsampled Pyramids (NSP) for multi-scale decomposition and Nonsubsampled Directional Filter Banks (NSDFB) for directional decomposition (Zhou et al., 2005; Dhavan & Garg, 2014; Singh et al., 2012; Tamilselvan & Murugesan, 2014; Janarthanan et al., 2018). Such expansion results in $k+1$ sub-images, which consist of one low- and high-frequency image having the same size as of the source image. NSP decomposition with $k=3$ level is shown in Figure 5. The equivalent filters of a k^{th} level cascading NSP are given in equation (4.2).

$$H_n^{\text{eq}}(z) = \begin{cases} H_1(z^{2^{n-1}}) \prod_{j=0}^{n-2} H_0(z^{2^j}) & 1 \leq n < k, \quad (4.2) \\ \prod_{j=0}^{n-2} H_0(z^{2^j}) & n = k + 1. \end{cases}$$

Figure 5(a) illustrates the 3-Stage nonsubsampled Pyramid Decomposition (Zhou et al., 2005). Four channel nonsubsampled directional filter bank and decomposition framework of the NSCT are given in the Figures 5(b) and (c) respectively. The equivalent filter in each channel is given in equation (4.3).

$$U_k^{\text{eq}}(z) = U_i(z) U_j(z^D) \quad (4.3)$$

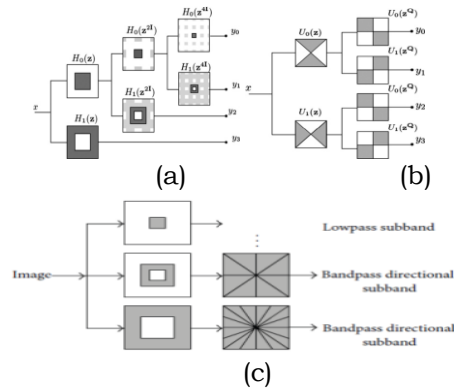


Fig 5. (a) 3-Stage Nonsubsampled Pyramid Decomposition (b). 4-channel Nonsubsampled directional filter bank (c) Decomposition framework of the NSCT

Steps of Fusion Algorithm

The steps of the proposed algorithms are given below:

- Read the input CT and MRI images.
- Find the required DTCWT for the source images individually.
- Apply NSCT for the above decomposed images individually.
- Apply Fusion rules.
- Do inverse transforms INSCT and IDTCWT on the fused image, to obtain the final fused image.

Evaluation Factors for Image Fusion

The following parameters are used to measure the fusion efficiency: (1) Average Difference (AD); (2) Maximum Difference (MD); (3) Root Mean Square Error (RMSE); (4) Standard Deviation (STD); (5) Peak Signal to noise Ratio (PSNR); (6) Entropy (H) and (7) Mutual Information (MI).

Results and Discussion

The calculated values of the parameters are compared with other existing techniques. Totally, 30 image pairs (CT and MRI) were taken for the analysis. Comparative analysis of one of the performance measurement factors, Average Difference (AD), suggests that it is minimized (4.62, 5.14, 5.23 and 5.86 for four sets of sample images respectively) while applying the proposed fusion technique. It is inferred that the maximum difference in proposed fusion technique is 68 for Set-1, for Set-2 it is 83, for Set-3 it is 67 and is 97 for Set-4 images. The effectiveness of the proposed fusion technique is also estimated with another parameter, Root Mean Square Error (RMSE), which should be minimum for the best fusion performance. RMSE obtained from this proposed model is 8.05(Set-1), 9.62(Set-2), 7.41(Set-3) and 10.03(Set-4). Another comparison is based on Standard Deviation (STD), it is 10.11 for the proposed technique for Set-1 images

which is also minimum. Similarly for Set-2, Set-3 and Set-4 images Standard Deviation is minimum (8.02, 10.15 and 9.93). The value of PSNR should be maximized in case of an effective image fusion technique. The measured value of PSNR for the proposed image fusion technique is 22.14 for Set-1 images. This is the maximum value among the simple, pyramid based and transforms based fusion techniques. PSNR for other techniques vary between 14.63 and 21.09.

Detection of Tumor from Real Time Clinical Images by using the proposed 3-HCAD System

In medical applications MR, CT and PET scans present identical values for lung and brain tumors. Therefore, in this research, MRI and CT images were taken for fusion. The efficiency of the proposed method is estimated by applying it on 30 clinical CT and MR images from patients (19 male and 11 female) with known or suspected tumors. These images were collected from a scan center at Erode, Tamil Nadu, India and from the Harvard Medical School website. Table 2 gives the details of different results obtained from this image set using the proposed 3-HCAD system.

Table 2
Performance Analysis with Real Time Images

Patient Number	Age/ Gender	Duration between CT- MRI	CT only	MRI only	3-HCAD result	Inconsistency
1	62/M	6	TP	TP	TP	-
2	58/F	2	TP	TP	TP	-
3	47/M	3	TP	TP	TP	-
4	51/M	5	TN	TN	TN	-
5	61/M	10	FP	TP	TP	+
6	36/M	9	TP	TP	TP	-
7	49/M	12	TN	TN	TN	-
8	54/F	4	FP	FP	FP	-
9	65/M	3	TN	TN	TN	-
10	55/M	7	TP	TP	TP	-
11	61/F	20	TP	TP	TP	-
12	72/M	6	FN	TP	TP	+
13	48/M	7	TP	TP	TP	-
14	34/F	2	TP	TP	TP	-
15	56/M	15	TP	TP	TP	-
16	63/M	1	TN	TN	TN	-
17	51/F	4	TP	TP	TP	-
18	74/M	9	TP	TP	TP	-
19	39/M	7	TN	TP	TP	+
20	68/M	3	TP	TP	TP	-
21	49/F	1	TP	TP	TP	-
22	66/M	14	TP	TP	TP	
23	71/M	21	TP	TP	TP	-
24	55/M	7	TP	TP	TP	-

25	52/M	2	TP	FN	TP	-
26	71/M	6	TP	TP	TP	-
27	47/M	4	TP	TP	TP	-
28	52/M	2	TP	TP	TP	-
29	28/M	16	TP	TP	TP	-
30	71/M	3	TP	TP	TP	-

Evaluation of Performance

The following performance measurement parameters are used for measuring the efficiency of the system:

- False positive (FP): Unaffected pixels detected
- False Negative (FN): Affected pixels not detected
- True Positive (TP): Affected pixels detected
- True Negative (TN): Unaffected pixels not detected
- Sensitivity: Ratio between TP and (TP+TN)
- Specificity: Ratio between TP and (TP+FP)
- Accuracy: Ratio between (TP+TN) and (TP+FP+FN+TN)
- Over all Error (OE): Sum of FP and FN
- False Positive Rate (FPR): Ratio of FP and (FN+FP)
- False Negative Rate (FNR): Ratio of FN and (FN+FP)

Result analysis and discussion

Fusion performance measurement parameters are shown in Table 3. From among stand-alone CT images, true-positive (TP) was for 23 patients, true-negative (TN) was for 4, false-negative (FN) was for 1 and false-positive (FP) was for 2 patients. From among stand-alone MRI images, TP was for 24 patients, TN was for 4, FP was for one and FN was for one patient. With the 3-HCAD system (CT and MRI), TP was for 25 patients (83.3%), TN was for 4 patients (16%) and FN was zero. The proposed 3-HCAD system showed sensitivity of 100%, accuracy of 96.66% and specificity of 96.25%.

Table 3
Diagnostic performance comparisons

Modality / Parameter	CT	MRI	3-HCAD [CT+MRI]
TP	23	24	25
TN	4	4	4
FP	2	1	1
FN	1	1	0
OE	3	2	1
FNR	4.16%	4%	0%
FPR	66.6%	50%	100%
Sensitivity	96.8%	96%	100%
Specificity	92%	96%	96.25%
Accuracy	90%	93.3%	96.66%

Performance comparison between existing fusion methods and 3-HCAD system is explained in Table 4. Graphical representation of the performance comparison of FPR, sensitivity, specificity and accuracy is presented in Figure 6. Although this proposal does not evaluate performance based on type of input imaging technique, CT imaging is preferred over MRI because of lower cost and ease of image acquisition using CT scanners. Also CT imaging gives more information that will help decision making in critical situations (Padma & Sukanesh, 2011; Gadpayleand & Mahajani, 2013).

Table 4
Performance comparisons between existing fusion method and 3-HCAD system

Fusion Technique	Sensitivity (%)	Specificity (%)	Accuracy (%)
Our Proposed Method (3-HCAD System)	100	96.25	96.66
KIFCM (EmanAbdel-Maksoud et al., 2015)	90.5	100	90.5
PCA+ANN (El-Sayed A. et al., 2014)	92.5	100	95
ZM+GLCM+SVM (Sumathi Ganesan et al., 2014)	90	94.51	94.23
DWT+PCA (Zhang et al., 2013)	97	96	95.5
SOM Clustering (Mehmood, Ejaz et al., 2013)	97.4	95.33	94.58

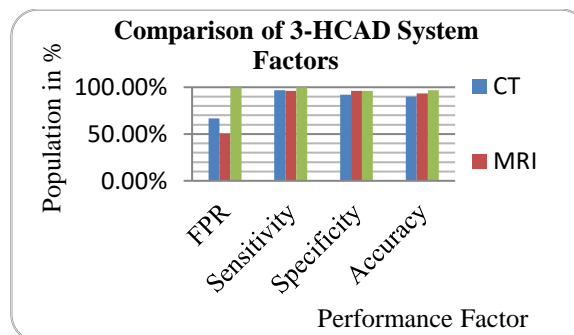


Fig 6. Comparison of Performance Factors

Conclusion

Innovations have been incorporated in image pre-processing, image segmentation and image fusion. This 3-stage Hybrid Computer Aided Design (3-HCAD) system's performance is compared with the existing systems using standard parameters such as sensitivity, specificity and accuracy and tested with real time clinical images. Results show that the 3-HCAD system provides 100% sensitivity and

96.66% accuracy, which are much higher than results of the other existing fusion methods. The real time implementation also ensures that the proposed 3-HCAD system enables the physician to conduct more detailed and exhaustive tests on patients in real time.

References

- Abdullah-Al-Wadud, M., Kabir, M. H., Dewan, M. A. A., & Chae, O. (2007). A dynamic histogram equalization for image contrast enhancement. *IEEE Transactions on Consumer Electronics*, 53(2), 593-600.
- Akbarzadeh Lari, M. R., Ghofrani, S., & McLernon, D. (2014). Using Curvelet transform for watermarking based on amplitude modulation. *Signal, Image and Video Processing*, 8(4), 687-697.
- AlZubi, S., Islam, N., & Abbod, M. (2011). Multiresolution analysis using wavelet, ridgelet, and curvelet transforms for medical image segmentation. *International journal of biomedical imaging*, 2011.
- Arizmendi, C., Vellido, A., & Romero, E. (2012). Classification of human brain tumours from MRS data using Discrete Wavelet Transform and Bayesian Neural Networks. *Expert Systems with Applications*, 39(5), 5223-5232.
- Aryani, L. N. A., & Lesmana, C. B. J. (2019). Neuropsychiatric factor and polymorphism gene in internet addiction. *International Journal of Health & Medical Sciences*, 2(1), 39-44. <https://doi.org/10.31295/ijhms.v2n1.90>
- Ashok, V., & Kumar, N. (2013). Determination of blood glucose concentration by using wavelet transform and neural networks. *Iranian journal of medical sciences*, 38(1), 51.
- Ashok, V., & Murugesan, G. (2017). Detection of retinal area from scanning laser ophthalmoscope images (SLO) using deep neural network. *International Journal of Biomedical Engineering and Technology*, 23(2-4), 303-314.
- Ashok, V., Karthik, R. P., Keerthana, K. M., & Roshinee, A. R. (2018, December). The Survival of Intellectual Disabled Subjects in Social Environment Using BCI. In *2018 International Conference on Intelligent Computing and Communication for Smart World (I2C2SW)* (pp. 181-184). IEEE.
- Ashok, V., Kumar, A. N., Kumar, S. S., & Kasthuri, N. (2010). Continuous wavelet transform analysis of blood flow for the determination of hyper and hypo glycemic conditions. *Procedia Computer Science*, 2, 291-297.
- Ashok, V., Nirmalkumar, A., & Jeyashanthi, N. (2011). A novel method for blood glucose measurement by noninvasive technique using laser. *International Journal of Biomedical and Biological Engineering*, 5(3), 113-119.
- Ashok, V., Nirmalkumar, A., Jeyashanthi, N. (2011). A novel method for blood glucose measurement by noninvasive technique using laser. *World Academy of Science, Engineering and Technology*, 51, pp. 676-682.
- Ashok, V., Rajan Singh, S., & Nirmalkumar, A. (2010). Determination of blood glucose concentration by back propagation neural network. *Indian Journal of Science and Technology*, 3(8), 916-18.
- Bai, Q., & Jin, C. (2015). IMAGE FUSION AND RECOGNITION BASED ON COMPRESSED SENSING THEORY. *International Journal on Smart Sensing & Intelligent Systems*, 8(1).
- Bauer, S., May, C., Dionysiou, D., Stamatakos, G., Buchler, P., & Reyes, M. (2011). Multiscale modeling for image analysis of brain tumor studies. *IEEE transactions on biomedical engineering*, 59(1), 25-29.

- Bhonsle, D., & Dewangan, S. (2012). Comparative Study of dual-tree complex wavelet transform and double density complex wavelet transform for Image Denoising Using Wavelet-Domain. *International Journal of Scientific and Research Publications*, 2(7), 1-5.
- Chang, S. G., Yu, B., & Vetterli, M. (2000). Adaptive wavelet thresholding for image denoising and compression. *IEEE transactions on image processing*, 9(9), 1532-1546.
- Chawla, M., Sharma, S., Sivaswamy, J., & Kishore, L. T. (2009, September). A method for automatic detection and classification of stroke from brain CT images. In *2009 Annual international conference of the IEEE engineering in medicine and biology society* (pp. 3581-3584). IEEE.
- Dhavan, R., & Garg, N. K. (2014). A hybrid approach of wavelets for effective image fusion for multimodal medical images. *International journal of technical research and application*, 2, 44-48.
- Dhillon, P. K., Mathur, P., Nandakumar, A., Fitzmaurice, C., Kumar, G. A., Mehrotra, R., ... & Dandona, L. (2018). The burden of cancers and their variations across the states of India: the Global Burden of Disease Study 1990–2016. *The Lancet Oncology*, 19(10), 1289-1306.
- Gadpayleand, P., & Mahajani, P. S. (2013). Detection and classification of brain tumor in MRI images. *International Journal of Emerging Trends in Electrical and Electronics*, IJETEE–ISSN, 2320-9569.
- Janarthanan, P. P., Ashok, V., Karthik, R. P., & Keerthana, K. M. (2018, December). Analysis on Behavioural Changes in the Intellectual Disability of the Individuals. In *2018 International Conference on Intelligent Computing and Communication for Smart World (I2C2SW)* (pp. 178-180). IEEE.
- Jeyashanthi, N., & Ashok, V. (2010). Anti-oxidative effect of *Cassia auriculata* on streptozotocin induced diabetic rats. *Indian Journal of Clinical Biochemistry*, 25(4), 429-434.
- Kumar, S., & Verma, P. (2012). Comparison of Different Enhanced Image Denoising with Multiple Histogram Techniques. *International of Soft Computing and Engineering (IJSCE)*, 2(2), 208-213.
- Mahidar, R. P., Prasad, N. V. G., & Sastry, V. L. N. (2011). A novel noisy image fusion technique using dual-tree complex wavelet transform. *International Journal of Engineering Science and Technology*, 3(6).
- Mitchell, H. B. (2010). *Image fusion: theories, techniques and applications*. Springer Science & Business Media.
- Om, H., & Biswas, M. (2012). An improved image denoising method based on wavelet thresholding.
- Padma, A., & Sukanesh, R. (2011). A wavelet based automatic segmentation of brain tumor in CT images using optimal statistical texture features. *International Journal of Image Processing*, 5(5), 552-563.
- Portilla, J., Strela, V., Wainwright, M. J., & Simoncelli, E. P. (2003). Image denoising using scale mixtures of Gaussians in the wavelet domain. *IEEE Transactions on Image processing*, 12(11), 1338-1351.
- Shreyamsha Kumar, B. K. (2015). Image fusion based on pixel significance using cross bilateral filter. *Signal, image and video processing*, 9(5), 1193-1204.
- Singh, R. P., Dwivedi, R. D., & Negi, S. (2012). Comparative Evaluation of DWT and DT-CWT for Image Fusion and De-noising. *International Journal of Applied Information Systems*, 4(2).

- Sivaranjani, S., Ashok, V., & Kumar, P. V. (2018). Data Scheduling for an Enhanced Cognitive Radio System in Healthcare Environment. *Current Trends In Biomedical Communication And Tele-Medicine*, 147.
- Sivaranjani, S., Ashok, V., Wahab, M.H.A., Jamil, M.M.B.A., Vinoth Kumar, P. (2019). Priority aware medical EEG data transmission using cognitive radio network. *International Journal of Control and Automation*, 12(6), pp. 364–370.
- Starck, J. L., Candès, E. J., & Donoho, D. L. (2002). The curvelet transform for image denoising. *IEEE Transactions on image processing*, 11(6), 670-684.
- Suryasa, I. W., Rodríguez-Gámez, M., & Koldoris, T. (2022). Post-pandemic health and its sustainability: Educational situation. *International Journal of Health Sciences*, 6(1), i-v. <https://doi.org/10.53730/ijhs.v6n1.5949>
- Tamilselvan, K. S., & Murugesan, G. (2014). Survey and analysis of various image fusion techniques for clinical CT and MRI images. *International journal of imaging systems and technology*, 24(2), 193-202.
- Vidyapeetham, A. V. (2010). An improved denoising algorithm using parametric multiwavelets for image enhancement. *SERSC International Journal of Advanced Science and Technology*, 16, 1-10.
- Yang, Y., Tong, S., Huang, S., & Lin, P. (2014). Log-Gabor energy based multimodal medical image fusion in NSCT domain. *Computational and mathematical methods in medicine*, 2014.
- Zhou, J., Cunha, A. L., & Do, M. N. (2005, September). Nonsubsampled contourlet transform: construction and application in enhancement. In *IEEE international conference on image processing 2005* (Vol. 1, pp. I-469). IEEE.